Journal of Maps, 2013
Vol. 9, No. 4, 505–512, http://dx.doi.org/10.1080/17445647.2013.820879

Routledge
Taylor & Francis Group

SCIENCE

Glacial geomorphology of the Tian Shan

Arjen P. Stroeven[a]*, Clas Hättestrand[a], Jakob Heyman[a,b], Johan Kleman[a] and Björn M. Morén[a]

[a]*Department of Physical Geography and Quaternary Geology, Stockholm University, Stockholm, Sweden;* [b]*Department of Earth, Atmospheric, and Planetary Sciences, Purdue University, West Lafayette, USA*

(*Received 21 November 2011; Resubmitted 10 May 2013; Accepted 27 June 2013*)

The glacial geomorphology of the Tian Shan has been mapped, with the study area covering almost 638,000 km^2. The map, designed to be printed at A0 size due to the elongated shape of the mountain range, is presented at a scale of 1:1,100,000. Five glacial landform categories are presented; glacial valleys, marginal moraines, glacial lineations, hummocky terrain and meltwater channels. These landform categories were mapped using the Shuttle Radar Topography Mission (SRTM) digital elevation model (90 m resolution), Landsat 7 ETM+ satellite imagery (30 m resolution), and images contained in Google Earth. The mapped landforms were created by glaciers that were restricted to mountain areas and their immediate surroundings.

Keywords: Tian Shan; glacial geomorphology; palaeoglaciology

1. Introduction

The Tian Shan (also called Tianshan and Tien Shan; 'celestial mountains' in Chinese) is a mountain range stretching from western China's Xinjiang Uyghur Autonomous Region in the east, to the northern Pamir Mountains, Kyrgyzstan, in the west. These mountains form part of mountainous Central Asia, along with, amongst others, the western Himalayas, Kunlun Shan, and the Altai Mountains (Figure 1). Kuhle (2004, and references therein) refers to scattered evidence in numerous publications from which he infers that a thick continuous ice mass covered the Tian Shan during the last glaciation (cf. Grosswald et al., 1994). However, most previous studies have focused on glacier extent and behaviour during the Holocene and the Little Ice Age (e.g. Bondarev et al., 1997; Meiners, 1997; Savoskul, 1997; Solomina et al., 2004). Recently, and with the advance of new radiometric dating techniques, local geomorphological mapping and dating of larger and older ice extents have flourished. Koppes et al. (2008), for example, investigated parts of the western Tian Shan in Kyrgyzstan and provided cosmogenic nuclide exposure age constraints for maximum ice extent that predated the Last Glacial Maximum (LGM). In contrast, Kong et al. (2009) published cosmogenic nuclide exposure ages from the eastern Tian Shan

*Corresponding author. Email: arjen.stroeven@natgeo.su.se

Figure 1. Overview of the mountainous regions of central Asia with the black box showing the map that covers the Tian Shan study area (638,000 km^2).

in China that are consistent with a maximum ice extent during the LGM. Xu et al. (2010) summarized these and other evidence for glaciations in the western and eastern Tian Shan during the Late Quaternary. Although such investigations across the Tian Shan have yielded local chronologies, a comprehensive picture of former glaciation across this important central Asian mountain range is lacking. With satellite imagery becoming more readily available, the ease and consistency with which mapping projects covering large areas can be conducted has increased. This mapping study is a first start towards a palaeoglaciological reconstruction of the Tian Shan and is an extension of previous work by Heyman et al. (2008, 2009, 2011), Stroeven et al. (2009) and Fu et al. (2012) for the eastern Tibetan Plateau margin. Large-scale mapping of glacial features, when combined with absolute age dating of key features, provides the foundation for reconstructing and modelling past glacier dynamics and provides spatial and temporal patterns of ice extent that can be used to constrain palaeoclimatic variations.

The study area covers ca. 638,000 km^2, encompassing most of the Tian Shan in China and in Kyrgyzstan (Figure 2). Two national capital cities (Bishkek, Kyrgyzstan; Almaty, Kazakhstan), and one regional capital (Ürümqi; Xinjian Uyghur Autonomous Region of China) are located within the mapped region. The Taklamakan Desert forms the south-eastern corner of the study area because the map is aligned W-E and the Tian Shan runs in a WSW-ENE direction.

2. Methods

The glacial geomorphology of the Tian Shan was mapped using the Shuttle Radar Topography Mission (SRTM) digital elevation model (DEM, 90 m horizontal resolution; Jarvis et al., 2008) and Landsat 7 Enhanced Thematic Mapper+ satellite imagery (Table 1; GLCF, 2009). The satellite imagery was compiled into false-colour composites of bands 5, 4, 2 (30 m resolution), and a semi-transparent grey-scale image of band 8 (15 m resolution), which is panchromatic, was used to sharpen the false-colour composites. To portray present-day glacier extents we use an enhanced

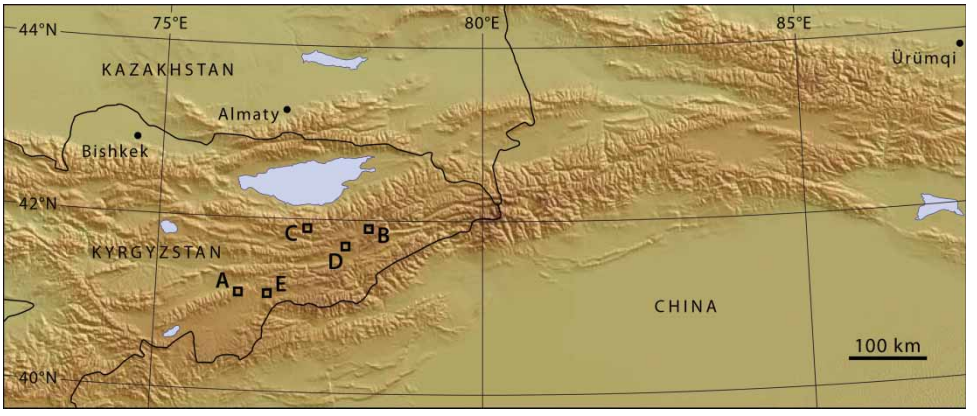

Figure 2. Map of the study area, with elevation, country borders, and major cities. A–E denote the location of landform examples shown in Figure 3.

version of the Randolph Glacier Inventory (Arendt et al., 2012), adopting revisions based on mapping in Google Earth. Mapping was primarily conducted at an on-screen scale of 1:100,000, and all landforms were mapped with various combinations of satellite imagery, DEM, and Google Earth for 3D visualisation. Field seasons in 2010 (eastern Tian Shan), 2011 and 2012 (eastern Kyrgyzstan) provided the opportunity to field check parts of the draft map.

Table 1. Landsat 7 ETM+ imagery used in this study to map the glacial geomorphology of the Tian Shan. All images were downloaded from GLCF (2009).

WRS Path	WRS Row	GLCF-ID	Acquisition date
142	30	039-188	1999-08-23
143	30	038-933	2000-09-17
144	30	038-976	2000-08-07
144	31	038-977	2000-08-07
145	29	039-020	1999-10-15
145	30	039-021	1999-10-15
145	31	039-022	2001-08-01
146	30	038-798	2000-08-05
146	31	038-799	2000-08-05
147	30	038-847	2000-09-13
147	31	038-848	2000-09-13
148	30	038-893	1999-09-18
148	31	038-894	1999-09-18
148	32	038-895	1999-09-18
149	30	038-640	1999-08-08
149	31	038-641	1999-09-09
149	32	038-642	1999-09-09
150	31	038-682	2001-08-20
150	32	038-683	2001-08-20
151	30	038-719	2001-06-08
151	31	038-720	2001-06-08
151	32	038-721	2000-08-24
152	31	038-758	2001-08-02

WRS, World Reference System.

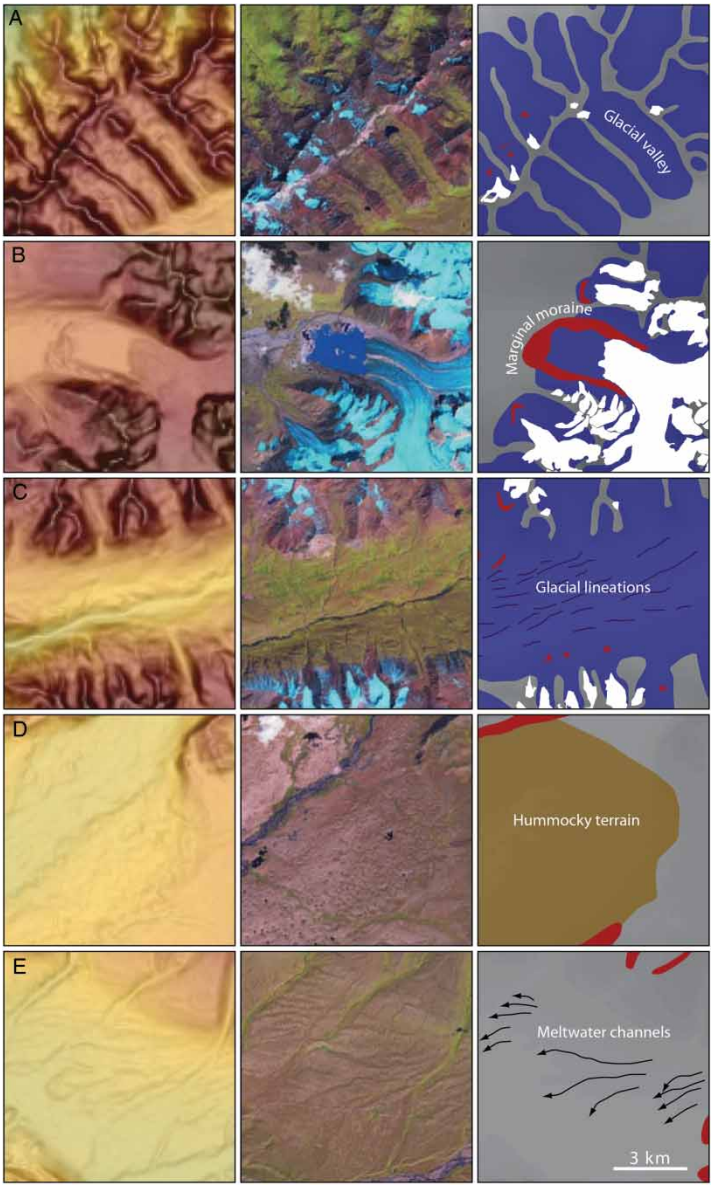

Figure 3. Landform examples with SRTM DEM panels (left), Landsat 7 ETM+ satellite imagery (middle), and mapped landforms (right). The DEM panels (left) are draped with a semi-transparent slope model in image A, and by a semi-transparent hillshade model in images B–E. The Landsat images (middle) are composites of bands 5, 4, 2, and are draped by a semi-transparent panchromatic image of band 8. North is towards the top of the panels and each panel is 9 × 9 km, see scale bar in panel E (right). (A) Glacial valleys oriented in a NW–SE direction. Note that contemporary glaciers are shown in light blue in the middle panel. (B) Marginal moraine deposited along the edge of a valley glacier. Note the lake dammed by the moraine in the middle panel. (C) Glacial lineations in a glacial valley. (D) Hummocky terrain. (E) Meltwater channels.

3. Landform descriptions

The landform categories and descriptions used in this study follow those presented for the eastern and central areas of the Tibetan Plateau (Heyman et al., 2008; Morén et al., 2011; Fu et al., 2012).

3.1. *Glacial valleys*

The glacial valley unit (Figure 3A) contains clearly U-shaped valleys and valleys with a trough-like shape (Graf, 1970). They have wide valley floors and truncated spurs. Glacial valleys occur in the high mountain areas and were cut by wet-based eroding glaciers flowing outwards and downwards towards surrounding lower terrain. In their lower reaches, the glacial valleys often transform to fluvial valleys characterised by linear slopes, V-shaped cross-valley profiles and a winding course with valley spurs. The transition from glacial- to fluvial cross-valley profiles can be identified using the profile tools in ESRI ArcGIS and Google Earth. The glacial valleys in the study area vary in size, with the largest being approximately 150 km long and 6 km wide, and the smallest about 1 km long and 0.5 km wide. Glacial valleys have primarily been identified using the DEM. Valleys with contemporary glaciers are included in the glacial valley category, although the valley profile is not visible.

3.2. *Marginal moraines*

Marginal moraines are deposited along stationary glacier margins and their locations, therefore, demarcate the former stillstands of the glaciers at a given time (Figure 3B; Small, 1983). In high mountain areas such as the Tian Shan, marginal moraines typically occur inside as well as outside of glacial valleys. In the latter case, they formed along the margins of piedmont lobes. Series of marginal moraines may belong to multiple glacial stages with successive maxima of similar but slightly shorter extent, or be part of the same stage and indicate stillstands during glacier retreat. The dimensions of the moraines in the study area range between c. 0.2 km and 18 km in length, and are up to 0.5 km in width. Marginal moraines have been identified on satellite imagery, Google Earth, and in the DEM.

3.3. *Glacial lineations*

Subglacially formed lineations, or glacial lineations (Figure 3C), are elongate landforms that can be highly diverse in dimensions and structure (Clark, 1997). They can consist solely of sediment or bedrock, or have a core of bedrock with a drape and tail of sediment (crag-and-tails). In the Tian Shan, glacial lineations are typically between 0.5 km and 3 km long. Field observations indicate that these are predominantly depositional features. Lineations usually occur inside glacial valleys, where wet-based ice has scoured the bedrock or deposited sediments. They have primarily been identified using the DEM and satellite imagery.

3.4. *Hummocky terrain*

Hummocky terrain consists of irregularly shaped mounds and depressions of sediments (Figure 3D; Eyles et al., 1999). The irregular landscape is in this area interpreted to be dead-ice topography, that is, the result of the uneven melting of an ice body and concentration of supraglacial debris in dead-ice depressions, ultimately forming mounds (Andersson, 1998). Although it is conceivable that hummocky terrain forms by other, subglacial, processes (Benn, 1992), a near-marginal genesis of the mapped hummocky terrain unit is corroborated by its proximity to the glacial valley and

marginal moraine units (compare with the definition of hummocky terrain in Heyman et al., 2008; Morén et al., 2011). The dimensions of the hummocky terrain areas are diverse, but are typically between 1 and 5 km across. Because hummocky terrain typically exhibits a gentle relief, it has been identified almost exclusively using satellite imagery and Google Earth.

3.5. *Meltwater channels*

Meltwater channels are channels eroded by marginal or pro-glacial meltwater and whose location and slope indicate that they formed close to or along a glacier margin (Figure 3E). These channels can therefore be used to reconstruct former ice-marginal positions (Mannerfelt, 1949). The meltwater channels in the Tian Shan are typically between 1 and 5 km long. Google Earth and the DEM have been the primary data sources for the identification of the study area's meltwater channels.

4. Conclusions

The glacial landform record of the Tian Shan, mapped and presented in this study, can usefully be employed towards a palaeoglaciological reconstruction. Marginal moraines indicate the presence of glacial advances of varying size and age (cf. Koppes et al., 2008; Xu et al., 2010). Glacial landforms occur mostly in the various massifs of the Tian Shan or in close proximity to them. Widespread areas of lower-lying terrain, despite careful inspection, were found to lack traces of glacial geomorphology. However, the method employed here has been shown to only yield a minimum extent of maximum glaciation (Heyman et al., 2009, 2011) and, for palaeoglaciological reconstructions, needs to be augmented with field investigations. For example, tills and erratic boulders might exist beyond the furthest limit of glaciation recorded by landforms (cf. Heyman et al., 2009). Landforms typically associated with ice sheet style glaciation, such as ribbed moraine, eskers, and drumlin swarms, were not found in the mapped area which indicates that only mountain glaciation has occurred in the Tian Shan range. Available radiometric dates seem to indicate that restricted glaciation occurred during the last glacial cycle (Koppes et al., 2008; Kong et al., 2009; Xu et al., 2010, and references therein).

Software

Satellite imagery was processed into false-colour composites in ENVI 4.3. These composites, together with the DEM, were imported into ESRI ArcGIS 10, in which the mapping was performed. Google Earth was used to visualize the area in a 3D environment. Adobe Illustrator was used to produce the final layout of the map.

Data

The authors have supplied data (as ESRI Shapefiles) used in the production of the accompanying map. These are available as Supplementary Materials.

Acknowledgements

The entire study area has been mapped by Morén while supervised by Hättestrand and Stroeven, and Heyman and Kleman added revisions to the mapping, in part guided by field observations of more extensive glacial extent than originally mapped. We acknowledge helpful reviews of Chris Clark, Amy Griffin, Jonathan Harbor, Matthias Kuhle and Mike Shand. Funding for this study was provided by the Swedish Research Council/Swedish International Development Cooperation Agency through their Swedish Research Links programme to Stroeven (348-2007-6924), by the Swedish Research Council to Stroeven (No. 2005-

4972) and an internationalisation grant of Stockholm University to Stroeven. This work was performed within the Bolin Centre for Climate Research environment.

References

Andersson, G. (1998). Genesis of hummocky moraine in the Bolmen area, southwestern Sweden. *Boreas*, *27*, 55–67. http://dx.doi.org/10.1111/j.1502-3885.1998.tb00867.x

Arendt, A., Bolch, T., Cogley, J. G., Gardner, A., Hagen, J-O, Hock, R., Kaser, G., Pfeffer, W. T., Moholdt, G., Paul, F., Radic, V., Andreassen, L., Bajracharya, S., Beedle, M., Berthier, E., Bhambri, R., Bliss, A., Brown, I., Burgess, E., Burgess, D., Cawkwell, F., Chinn, T., Copland, L., Davies, B., De Angelis, H., Dolgova, E., Filbert, K., Forester, R., Fountain, A., Frey, H., Giffen, B., Glasser, N., Gurney, S., Hagg, W., Hall, D., Haritashya, U. K., Hartmann, G., Helm, C., Herreid, S., Howat, I., Kapustin, G., Khromova, T., Kienholz, C., Koenig, M., Kohler, J., Kriegel, D., Kutuzov, S., Lavrentiev, I., LeBris, R., Lund, J., Manley, W., Mayer, C., Miles, E., Li, X., Menounos, B., Mercer, A., Moelg, N., Mool, P., Nosenko, G., Negrete, A., Nuth, C., Pettersson, R., Racoviteanu, A., Ranzi, R., Rastner, P., Rau, F., Raup, B. H., Rich, J., Rott, H., Schneider, C., Seliverstov, Y., Sharp, M., Sigurðsson, O., Stokes, C., Wheate, R., Winsvold, S., Wolken, G., Wyatt, F., & Zheltyhina, N. (2012). Randolph Glacier Inventory [v2.0]: A dataset of global glacier outlines. Global Land Ice Measurements from Space, Boulder Colorado, USA. Digital Media.

Benn, D. I. (1992). The genesis and significance of 'hummocky moraine': Evidence from the Isle of Skye, Scotland. *Quaternary Science Reviews*, *11*, 781–799. Retrieved from http://dx.doi.org/10.1016/0277-3791(92)90083-K

Bondarev, L. G., Gobedzhishvili, R. G., & Solomina, O. S. (1997). Fluctuations of local glaciers in the southern ranges of the former USSR: 18,000–8000 BP. *Quaternary International*, *38/39*, 103–108. Retrieved from http://dx.doi.org/10.1016/S1040-6182(96)00023-7

Clark, C. D. (1997). Reconstructing the evolutionary dynamics of former ice sheets using multi-temporal evidence, remote sensing and GIS. *Quaternary Science Reviews*, *16*, 1067–1092. Retrieved from http://dx.doi.org/10.1016/S0277-3791(97)00037-1

Eyles, N., Boyce, J. J., & Barendregt, R. W. (1999). Hummocky moraine: Sedimentary record of stagnant Laurentide Ice Sheet lobes resting on soft beds. *Sedimentary Geology*, *123*, 163–174. Retrieved from http://dx.doi.org/10.1016/S0037-0738(98)00129-8

Fu, P., Heyman, J., Hättestrand, C., Stroeven, A. P., & Harbor, J. M. (2012). Glacial geomorphology of the Shaluli Shan area, southeastern Tibetan Plateau. *Journal of Maps*, *8*, 48–55, Retrieved from http://dx.doi.org/10.1080/17445647.2012.668762

GLCF. (2009). *Global Land Cover Facility*. Retrieved February 10, 2011, from http://glcf.umiacs.umd.edu

Graf, W. L. (1970). The geomorphology of the glacial valley cross section. *Arctic and Alpine Research*, *2*, 303–312. Retrieved from http://dx.doi.org/10.2307/1550243

Grosswald, M. G., Kuhle, M., & Fastook, J. L. (1994). Würm glaciation of Lake Issyk-Kul area, Tian Shan Mts.: A case study in glacial history of Central Asia. *GeoJournal*, *33*, 273–310. Retrieved from http://dx.doi.org/10.1007/BF00812878

Heyman, J., Hättestrand, C., & Stroeven, A. P. (2008). Glacial geomorphology of the Bayan Har sector of the NE Tibetan Plateau. *Journal of Maps*, *v2008*, 42–62. Retrieved from http://dx.doi.org/10.4113/jom.2008.96

Heyman, J., Stroeven, A. P., Alexanderson, H., Hättestrand, C., Harbor, J., Li, Y. K., Caffee, M. W., Zhou, L. P., Veres, D., Liu, F., & Machiedo, M. (2009). Palaeoglaciation of Bayan Har Shan, northeastern Tibetan Plateau: Glacial geology indicates maximum extents limited to ice cap and ice field scales. *Journal of Quaternary Science*, *24*, 710–727. Retrieved from http://dx.doi.org/10.1002/jqs.1305

Heyman, J., Stroeven, A. P., Caffee, M. W., Hättestrand, C., Harbor, J. M., Li, Y. K., Alexanderson, H., Zhou, L. P., & Hubbard, A. (2011). Palaeoglaciology of Bayan Har Shan, NE Tibetan Plateau: Exposure ages reveal a missing LGM expansion. *Quaternary Science Reviews*, *30*, 1988–2001. Retrieved from http://dx.doi.org/10.1016/j.quascirev.2011.05.002

Jarvis, A., Reuter, H. I., Nelson, A., & Guevara, E. (2008). Hole-filled seamless SRTM data V4. Retrieved February 10, 2011, from http://srtm.csi.cgiar.org/

Kong, P., Fink, D., Na, C., & Huang, F. (2009). Late quaternary glaciation of the Tianshan, central Asia, using cosmogenic ^{10}Be surface exposure dating. *Quaternary Research*, *72*, 229–233. Retrieved from http://dx.doi.org/10.1016/j.yqres.2009.06.002

Koppes, M., Gillespie, A. R., Burke, R. M., Thompson, S. C., & Stone, J. (2008). Late quaternary glaciations in the Kyrgyz Tien Shan. *Quaternary Science Reviews*, *27*, 846–866. Retrieved from http://dx.doi.org/10.1016/j.quascirev.2008.01.009

Kuhle, M. (2004). The high glacial (Last Ice Age and LGM) ice cover in high and Central Asia. *Developments in Quaternary Science*, *2c*, 175–199. Retrieved from http://dx.doi.org/10.1016/S1571-0866(04)80123-4

Mannerfelt, C. M. (1949). Marginal drainage channels as indicators of the gradients of Quaternary ice caps. *Geografiska Annaler*, *31*, 194–199. Retrieved from http://dx.doi.org/10.2307/520362

Meiners, S. (1997). Historical to post glacial glaciation and their differentiation from the late glacial period on examples of the Tian Shan and the N.W. Karakorum. *GeoJournal*, *42*, 259–302. Retrieved from http://dx.doi.org/10.1023/A:1006817422505

Morén, B., Heyman, J., & Stroeven, A. P. (2011). Glacial geomorphology of the central Tibetan Plateau. *Journal of Maps*, *v2011*, 115–125. Retrieved from http://dx.doi.org/10.4113/jom.2011.1161

Savoskul, O. S. (1997). Modern and little ice age glaciers in 'humid' and 'arid' areas of the Tien Shan, Central Asia: two different patterns of fluctutation. *Annals of Glaciology*, *24*, 142–147.

Small, R. J. (1983). Lateral moraines of Glacier De Tsidjiore Nouve: Form, development, and implications. *Journal of Glaciology*, *29*, 250–259. Retrieved from http://www.igsoc.org/journal/29/

Solomina, O., Barry, R., & Bodnya, M. (2004). The retreat of Tien Shan glaciers (Kyrgyzstan) since the little ice age estimated from aerial photographs, lichenometric and historical data. *Geografiska Annaler*, *86A*, 205–215. Retrieved from http://dx.doi.org/10.1111/j.0435-3676.2004.00225.x

Stroeven, A. P., Hättestrand, C., Heyman, J., Harbor, J., Li, Y. K., Zhou, L. P., Caffee, M. W., Alexanderson, H., Kleman, J., Ma, H. Z., & Liu, G. N. (2009). Landscape analysis of the Huang He headwaters, NE Tibetan Plateau – patterns of glacial and fluvial erosion. *Geomorphology*, *103*, 212–226. Retrieved from http://dx.doi.org/10.1016/j.geomorph.2008.04.024

Xu, X., Kleidon, A., Miller, L., Wang, S., Wang, L., & Dong, G. (2010). Late quaternary glaciations on the Tianshan and implications for palaeoclimatic change: A review. *Boreas*, *39*, 215–232. Retrieved from http://dx.doi.org/10.1111/j.1502-3885.2009.00118.x